Eur. Phys. J. B **15**, 51–57 (2000)

THE EUROPEAN PHYSICAL JOURNAL B

EDP Sciences

Noise-induced bifurcations and chaos in the average motion of globally-coupled oscillators

Ying Zhang[1], Gang Hu[2,3], Shi Gang Chen[1], and Yugui Yao[4,a]

[1] LCP, Institute of Applied Physics and Computational Mathematics, PO Box 8009(26), Beijing 100088, P.R. China
[2] CCAST (World Laboratory), PO Box 8730, Beijing 100080, P.R. China
[3] Physics Department, Beijing Normal University, Beijing 100875, P.R. China
[4] State Key Laboratory for Surface Physics, Institute of Physics & Center for Condensed Matter Physics, PO Box 603-4-0, Beijing 100080, P.R. China

Received 6 April 1999 and Received in final form 1 November 1999

Abstract. A system of coupled master equations simplified from a model of noise-driven globally coupled bistable oscillators under periodic forcing is investigated. In the thermodynamic limit, the system is reduced to a set of two coupled differential equations. Rich bifurcations to subharmonics and chaotic motions are found. This behavior can be found only for certain intermediate noise intensities. Noise with intensities which are too small or too large will certainly spoil the bifurcations. In a system with large though finite size, the bifurcations to chaos induced by noise can still be detected to a certain degree.

PACS. 05.45.-a Nonlinear dynamics and nonlinear dynamical systems – 05.40.-a Fluctuation phenomena, random processes, noise, and Brownian motion

1 Introduction

The presence of noise or computer round off are ubiquitous in physical experiments and computer simulations and the study of their effects is of fundamental importance. From an intuitive point of view, noise spoils signals, and gives rise to various randomness and disorders. However, in the last two decades we have become aware of the active role of noise for enhancing coherence, signal and order. Most of the work on this aspect has focused on the stochastic resonance (SR) effect [1–11]. There exists another also widely accepted concept on noise; that noise rules out fine structures and various bifurcations. For instance, for period-doubling bifurcations appearing in nonlinear systems, noise can definitely wash out high periodicities. Can we find the opposite case, *i.e.*, the active role played by noise in inducing structures and does there exist a certain optimal noise for this active effect? In this paper, we investigate this subject; a huge variety of bifurcations to subharmonics, quasiperiodicities and chaos are found to be induced by noise, and this is identified for a certain medium range of noise. In Section 2 we describe our model, starting from a two-series globally-coupled oscillator forced by uncorrelated white noise and periodic forcing (Eqs. (2)). The continuous system is reduced to globally-coupled master equations in the small limit of noise and forcing (Eqs. (4)). In Section 3, the coupled master equations are further reduced to a set of two ordinary differential equations in the infinite size limit. We find, in simulations, rich behavior of noise-induced subharmonics, chaos and bifurcations among these different types of motions for medium noise intensity. In Section 4, we numerically compute the coupled master equations (Eqs. (4)) and the original coupled continuous bistable oscillators (Eqs. (2)). Noise-induced bifurcations to subharmonics and chaos can be also clearly traced, qualitatively reproducing the essential features of the simplified system. However, quantitative deviations between these equations are relatively large since the parameter regions where we find the complex structures are far beyond the justification of our approximation for the reduction of the equations. A brief conclusion is given in the last section.

2 Model

We consider a model of globally coupled two-series cells which are indicated by (x_i, y_i), $i = 1, 2, \ldots N$. The inner dynamics of each cell is described by

$$\begin{aligned} \dot{x} &= ax - x^3 + \Gamma(t), \\ \dot{y} &= y - y^3 + \Delta(t), \end{aligned} \tag{1}$$

where $a > 0$, $\Gamma(t)$ and $\Delta(t)$ are white noises. While all the cells are under periodic forcing $A\cos(\omega t)$, they are globally coupled with each other through a single

[a] e-mail: ygyao@aphy.iphy.ac.cn

quantity $Z = X - Y$ as

$$\begin{aligned}
\dot{x}_i &= ax_i - x_i^3 + \mu_1 Z(t) + A\cos(\omega t) + \Gamma_i(t) \\
\dot{y}_j &= y_j - y_j^3 + \mu_2 Z(t) + A\cos(\omega t) + \Delta_i(t) \\
\langle \Gamma_i(t)\rangle &= 0, \langle \Gamma_i(t)\Gamma_{i'}(t')\rangle = 2D_1\delta_{ii'}\delta(t-t') \\
\langle \Delta_j(t)\rangle &= 0, \langle \Delta_j(t)\Delta_{j'}(t')\rangle = 2D_2\delta_{jj'}\delta(t-t') \\
\langle \Gamma_i(t)\Delta_j(t')\rangle &= 0
\end{aligned} \tag{2}$$

where $X = \frac{1}{N}\sum_{i=1}^{i=N} x_i$, $Y = \frac{1}{N}\sum_{j=1}^{j=N} y_j$, and x_i are regarded being active, y_i are suppressive. The competition between x and y yields many interesting features of this model. In equations (2) we take $a = 0.9$, $\omega = 0.009016$, $\mu_2 = \beta\mu_1 = \beta\mu$, $\beta = 0.6$ and $D_1 = D_2 = D$ throughout the paper. Throughout the following, we investigate the macroscopic state in phase space $(X(t), Y(t))$ which shows the average behavior of the microscopic variables $(x_1, y_1; ...; x_N, y_N)$. The positive couplings in equations (2) can be also regarded as the diffusive couplings, and the negative ones as resistance-like couplings. It is interesting to investigate the effect caused by their interactions. For (2) our theoretical analysis is based on the conditions

$$\mu,\ A,\ \omega,\ D \ll 1 \qquad \text{and} \qquad N \gg 1. \tag{3}$$

The inequality $\mu, A, \omega \ll 1$ guarantees bistability of each x_i and y_j in the system (2).

Under the condition (3), the continuous bistable systems (2) can be reduced to two-state systems for x_i and y_j respectively, and then the coupled stochastic bistable systems can be simplified to the following coupled master equations [12]

$$\begin{aligned}
\dot{P}^{\pm}_{x_i} &= -R_x P^{\pm}_{x_i} + R^{\mp}_x \\
\dot{P}^{\pm}_{y_j} &= -R_y P^{\pm}_{y_j} + R^{\mp}_y \\
P^{+}_{x_i} + P^{-}_{x_i} &= 1,\ i = 1, 2, ..., N \\
P^{+}_{y_j} + P^{-}_{y_j} &= 1,\ j = 1, 2, ..., N
\end{aligned} \tag{4}$$

where $P^{+}_{x_i}$ and $P^{-}_{x_i}$ ($P^{+}_{y_j}$ and $P^{-}_{y_j}$) are the probabilities for x_i (y_j) to take the state $+\sqrt{a}$ and $-\sqrt{a}$ ($+1$ and -1) respectively; R^{+}_x (R^{-}_x) is the transition rate from state $+\sqrt{a}$ to $-\sqrt{a}$ ($-\sqrt{a}$ to $+\sqrt{a}$) for x, and R^{+}_y (R^{-}_y) is that from $+1$ to -1 (-1 to $+1$) for y, which are:

$$\begin{aligned}
R^{\pm}_x &= \frac{a}{\sqrt{2}\pi}\exp\left(-\frac{a^2}{4D} \mp \frac{\sqrt{a}(\mu Z + A\cos(\omega t))}{D}\right), \\
R_x &= R^{+}_x + R^{-}_x = r_{01}\cosh\left(\frac{\sqrt{a}(\mu Z + A\cos(\omega t))}{D}\right), \\
R^{\pm}_y &= \frac{1}{\sqrt{2}\pi}\exp\left(-\frac{1}{4D} \mp \frac{\beta\mu Z + A\cos(\omega t)}{D}\right), \\
R_y &= R^{+}_y + R^{-}_y = r_{02}\cosh\left(\frac{\beta\mu Z + A\cos(\omega t)}{D}\right), \\
r_{01} &= \frac{a\sqrt{2}}{\pi}\exp\left(-\frac{a^2}{4D}\right), \\
r_{02} &= \frac{\sqrt{2}}{\pi}\exp\left(-\frac{1}{4D}\right).
\end{aligned} \tag{5}$$

In reference [13], we took $A = 0$, and considered the average behavior of the system. The global variables $(X(t), Y(t))$ of the system show three types of phases of average motion under the condition $N \to \infty$; one of them is the oscillation phase. In references [14,15], we studied the case with periodic forcing. Noise-induced Hopf bifurcation was revealed, and stochastic resonance was found which was sensitively dependent on the frequency of the external forcing. In this paper, we start from the same model described by equations (2, 3), but further investigate the possibility of noise-induced bifurcations to various subharmonics and chaos.

In the following we will focus on the master equations (4) rather than equations (2). On the one hand, the derivation and theory from equations (2–4) under the condition (3) are well-established. On the other hand, equations (4) are practically important in their own right for describing globally coupled two-state spin systems. Moreover, the numerical computation for equations (4) is considerably simpler than that for equations (2) for the very large N values needed to explore fully the rich complexities. Then in the following sections, we study equations (4) only, and release the constraints of equations (3) for linking equations (2, 4), and freely consider a much wider region for D and μ. Nevertheless, a brief discussion of the original equations (2) will be also presented at the end of Section 4.

3 Noise-induced subharmonics and chaos for an infinite system

By averaging equations (4)

$$\begin{aligned}
\langle X(t)\rangle &= \frac{1}{N}\sum_{i=1}^{N}[\sqrt{a}P^{+}_{x_i} + (-\sqrt{a})P^{-}_{x_i}] \\
\langle Y(t)\rangle &= \frac{1}{N}\sum_{j=1}^{N}[P^{+}_{y_j} + (-1)P^{-}_{y_j}]
\end{aligned} \tag{6}$$

we can reduce the N coupled master equations (4) to a set of two-dimensional differential equations

$$\begin{aligned}
\dot{\langle X(t)\rangle} &= -r_{01}\cosh\left(\frac{\sqrt{a}(\mu Z + A\cos(\omega t))}{D}\right)\langle X(t)\rangle \\
&\quad + \sqrt{a}r_{01}\sinh\left(\frac{\sqrt{a}(\mu Z + A\cos(\omega t))}{D}\right) \\
\dot{\langle Y(t)\rangle} &= -r_{02}\cosh\left(\frac{\beta\mu Z + A\cos(\omega t)}{D}\right)\langle Y(t)\rangle \\
&\quad + r_{02}\sinh\left(\frac{\beta\mu Z + A\cos(\omega t)}{D}\right).
\end{aligned} \tag{7}$$

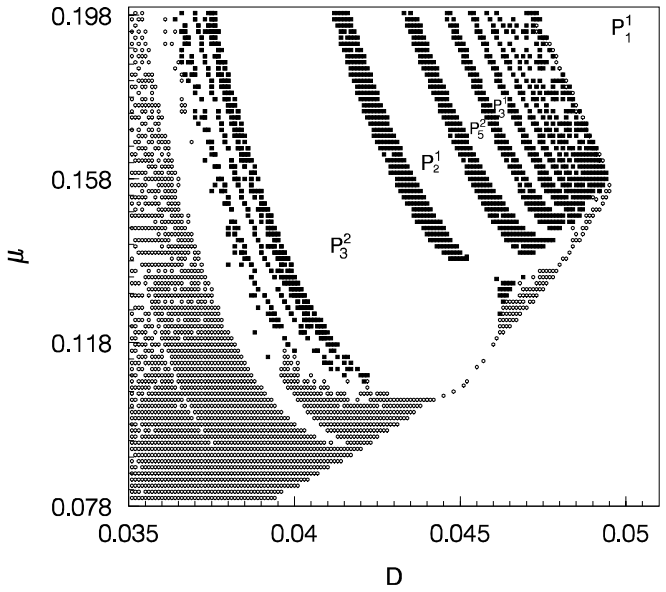

Fig. 1. Different phases of the Farey tree distributed in the $D-\mu$ parameter plane. $A = 0.045$. Squares indicate chaos, circles indicate quasiperiodicity, and the others represent periodic regions. The marks P_m^n signify the period m of the motion (m times of the period of the driving force), which makes $(m-n)$ circles in each period.

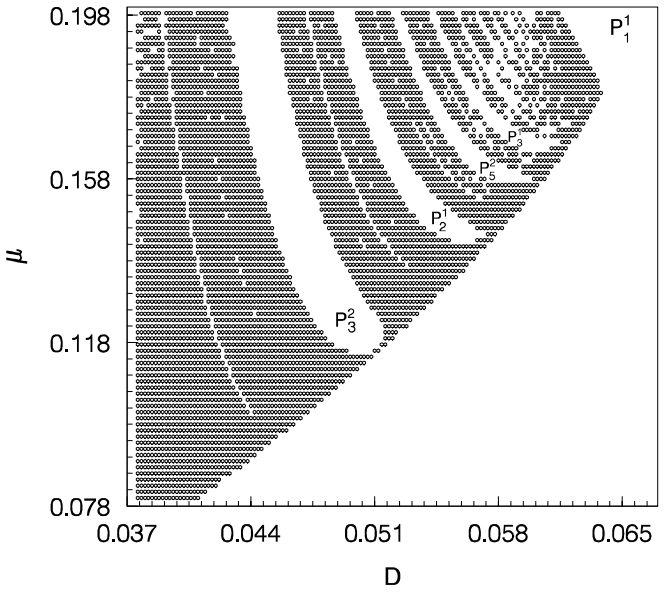

Fig. 2. The same as Figure 1 with $A = 0.0075$; no chaos exists.

In the thermodynamic limit $N \to \infty$, $X(t) = \langle X(t)\rangle$ and $Y(t) = \langle Y(t)\rangle$; we have

$$\begin{aligned}
\dot{X}(t) &= -r_{01}\cosh\left(\frac{\sqrt{a}(\mu Z + A\cos(\omega t))}{D}\right)X(t) \\
&\quad + \sqrt{a}r_{01}\sinh\left(\frac{\sqrt{a}(\mu Z + A\cos(\omega t))}{D}\right) \\
\dot{Y}(t) &= -r_{02}\cosh\left(\frac{(\beta\mu Z + A\cos(\omega t))}{D}\right)Y(t) \\
&\quad + r_{02}\sinh\left(\frac{(\beta\mu Z + A\cos(\omega t))}{D}\right) \\
Z(t) &= X(t) - Y(t). \qquad (8)
\end{aligned}$$

Thus, the high-dimensional master equations (4) with an infinite system size are reduced to a set of two-dimensional coupled differential equations (8).

Now we focus on the dynamics of $(X(t), Y(t))$. Figure 1 illustrates the phase space $\mu - D$ with periodic forcing fixed at $A = 0.045$. The squares in Figure 1 denote chaos, the circles correspond to quasiperiodicity, and the blank regions mean periodic motions of the system, where P_m^n indicates that the system on the left edge of the given zone has periodic trajectories of period mT, which runs at an angle of $(m-n)*2\pi$ around the center of the coordinate system $(X(t), Y(t))$ in each period (T means the period of the driving force, and equals to $\frac{2\pi}{\omega}$). This motion will be followed by a period-doubling cascade in the same zone.

For very small D the system behaves with a quasiperiodic oscillation, which is typical for a limit cycle system [13] subject to a periodic forcing. For very large D, the motion is a periodic oscillation with the same frequency as the forcing, which is expected for a fixed point system [13] subject to a periodic forcing. The behaviors for both large and small D are simple, while, for medium D, the system shows very rich and interesting noise-induced transitions, and has many complex structures. The optimal noise for rich bifurcations and patterns can be regarded as a kind of stochastic resonance for generating complexity.

Detailed simulation shows that the chaotic system bifurcates into periodic windows through inverse tangent bifurcation, and various windows appear in an order of Farey tree as P_3^2, P_2^1, P_5^2, P_3^1, P_7^2, P_4^1, P_9^2, P_5^1, P_{11}^2, P_6^1, P_{13}^2, P_7^1, P_{15}^2, P_8^1... In Figure 2 we repeat as for Figure 1, but for smaller periodic forcing $A = 0.0075$, then one can no longer see chaos. Apart from the large P_1^1 region we find only a quasiperiodicity "sea" containing various periodic "tongues". Figures 3–5 take some examples for some branches of the Farey tree, chaos, and quasiperiodicity in Figure 1, with μ fixed at 0.16 and D varied. Figures 3a–f show orbits of P_3^2, P_2^1, P_5^2, P_3^1, chaos, and quasiperiodic motion, respectively. Figures 4a–f are their strobe plots, in which $(X(t),Y(t))$ are plotted at times $t = nT$ with n being large positive integers, while Figures 5a–f present the corresponding frequency spectra. Coexistence of multiple attractors can be observed in certain regions.

We compute the largest Lyapunov exponents of the system *vs.* D for $\mu = 0.16$ in Figure 6a, and *vs.* μ for $D = 0.045$ in Figure 6b. The largest positive Lyapunov exponent refers to the squared chaotic subregions in Figure 1, and the zero Lyapunov exponent corresponds to the circled quasiperiodic subregions. Figure 6a shows clearly that the Farey tree will grow into an infinite period at certain finite accumulation parameter point. This period cannot, however, be identified due to our finite precision. Quasiperiodicity can be seen easily for both small D ($D < 0.0365$, and one example in Figs. 3f, 4f and 5f)

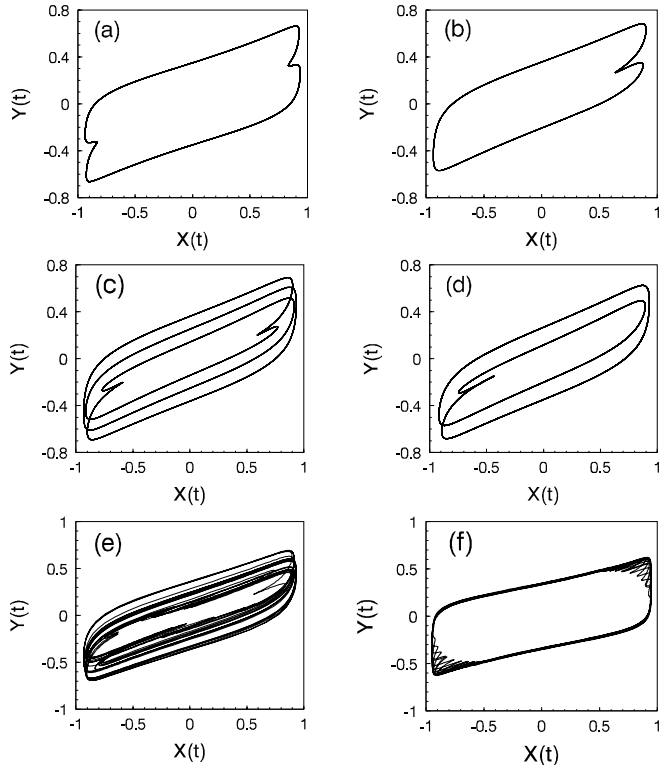

Fig. 3. Orbits of different types of motion of equation (8). $\mu = 0.16$, $D = 0.04$, 0.0445, 0.046, 0.0472, 0.04564 and 0.036 in (a–f), and the motions observed are P_3^2, P_2^1, P_5^2, P_3^1, chaos, and quasiperiodicity, respectively.

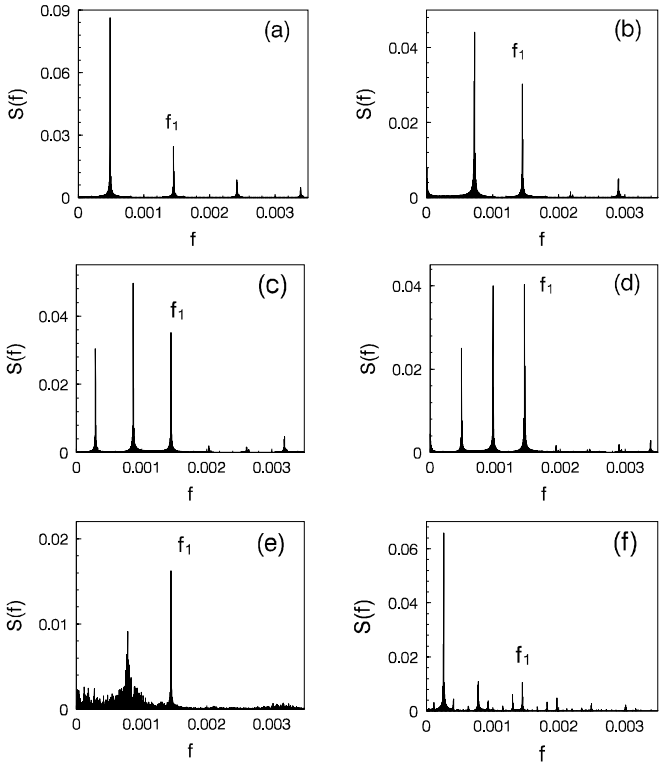

Fig. 5. Frequency spectra corresponding to Figure 3 where f_1 is the frequency of the driving force $f_1 = \frac{\omega}{2\pi}$.

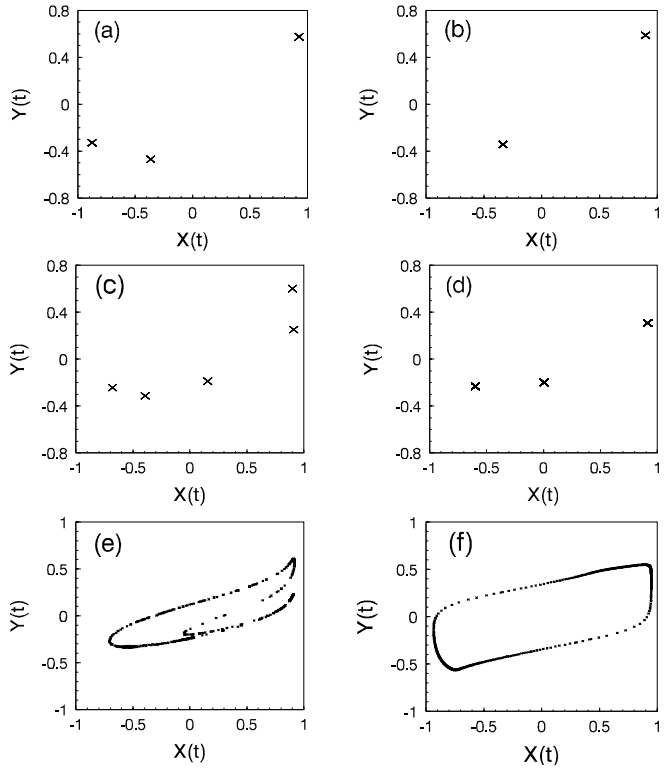

Fig. 4. Strobe plots corresponding to Figure 3.

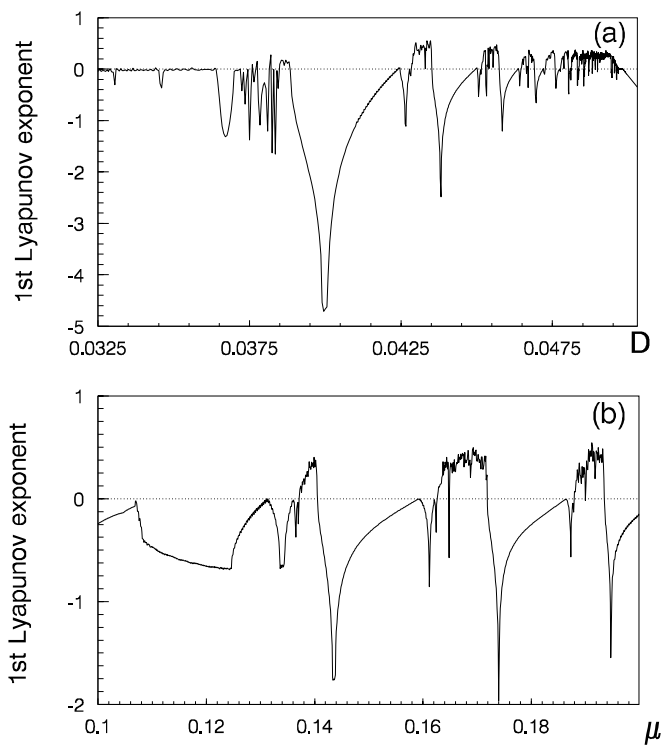

Fig. 6. (a) The maximum Lyapunov exponent λ_m *vs.* D with μ fixed at 0.16. (b) The maximum Lyapunov exponent λ_m *vs.* μ with D fixed at 0.045.

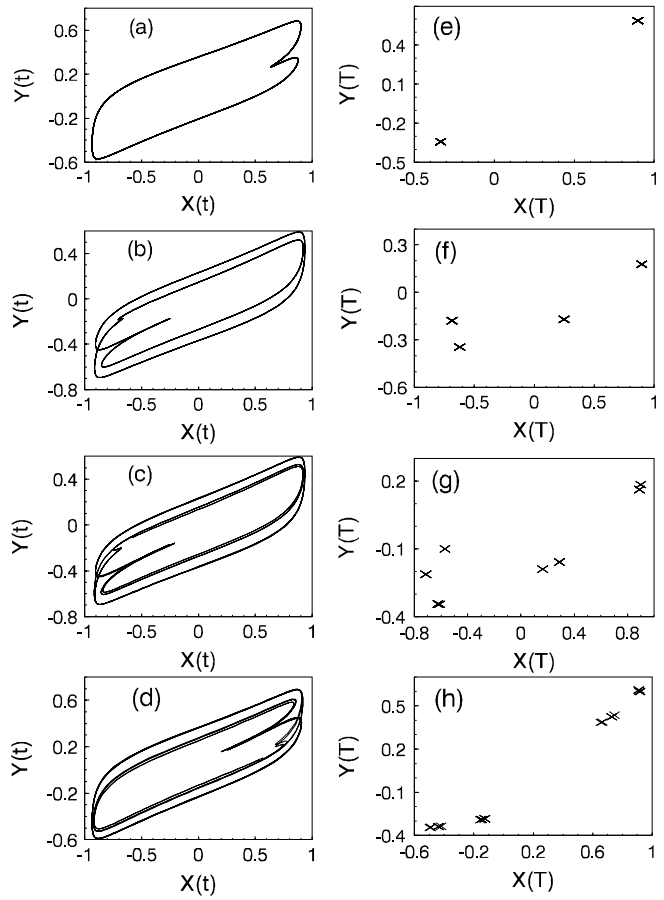

Fig. 7. (a–d) Orbits P_2^1 in (a) and its period-doublings; P_4^2 in (b), P_8^4 in (c), and P_{16}^8 in (d). $\mu = 0.16$, and D is 0.04450 for (a); 0.04510 for (b); 0.045140 for (c); and 0.045150 for (d). (e–h): Strobe plots corresponding to (a–d), respectively.

and large D ($0.0496 < D < 0.0499$) regions, depending on the largest Lyapunov exponent remaining on zero. We can find quasiperiodicity to chaos in the boundary of the corresponding parameter regions.

On the other hand, in each periodic window of the Farey tree one can find a period-doubling cascade leading to chaos. Figure 7 gives some examples for the periodic doubling bifurcation route in the P_2^1 window referring to Figure 1 and in the interval of $0.0435 < D < 0.0452$ in Figure 6a. In Figure 7, we have $\mu = 0.16$, and (a–d) are orbits of P_2^1, P_4^2, P_8^4, and P_{16}^8, while (e–h) are their strobe plots, respectively.

In brief, it is clear that the system motion is rather simple either for very small or rather large D; rich bifurcations to various subharmonics and chaos can be observed only in a certain intermediate range of D as far as driving force A (not too weak) and infinite system size limits are concerned. Therefore, the most complicated bifurcation figure appears in a certain intermediate region of noise intensity, this reminds us of an analog of stochastic resonance in producing a complexity to the average motion of the extended system.

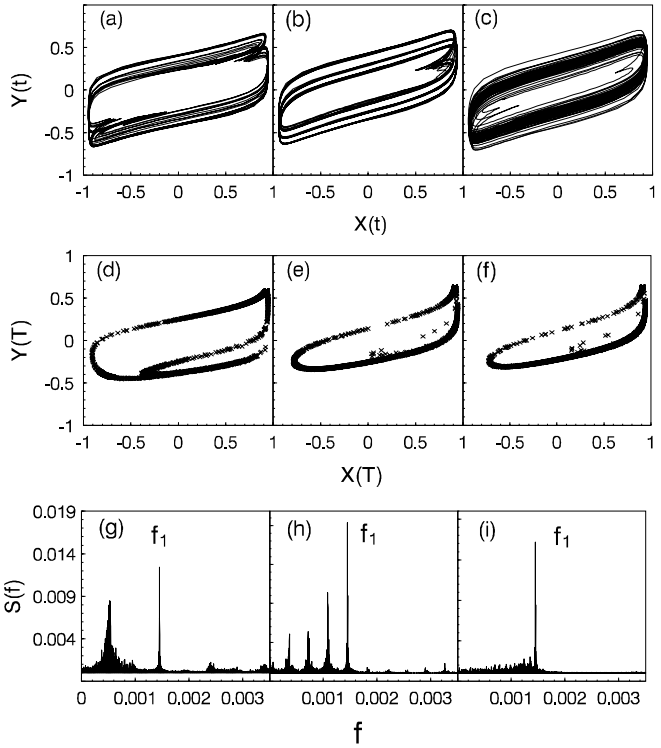

Fig. 8. (a–c) Orbits from the simulation of equations (4). (d–f) Strobe plots corresponding to (a–c). (g–i) Frequency spectra corresponding to (a–c). $N = 30$, and all other parameters of (a–c) are the same as those of Figures 3 (a–c), respectively.

4 Numerical results for coupled systems with finite system size

All the above results are obtained from equations (8), which are valid for the thermodynamic limit, $N \to \infty$. Realistically, any system has finite system size, and it is necessary to study the finite system size effect. In particular, we should investigate whether the noise-induced rich structures can survive for finite system size. For instance, it is interesting to study to what extent the two-dimensional equations (8) can well represent the original N coupled master equations (4), and for how large N the bifurcation figures of Figures 3–5 can be reproduced for the large noise system. Now we will directly investigate equations (4) for different N with all other parameters being taken the same as (a–c) of Figures 3–5, and compare the results with those from equations (8).

First, we set the system size to a very small value, and Figure 8 shows an example with $N = 30$. Then we find random motion only, which is trivial behavior for a periodically driven noisy system, and no any trace for various complexities is evident except a small tail of subharmonics in the spectra, for example $\frac{1}{3}f_1$ in Figure 8g and $\frac{1}{4}f_1$ in Figure 8h. By increasing the system size to a medium value (*e.g.*, $N = 100$), various subharmonics appear. In Figure 9, we can observe P_3^2 clearly in the trajectory of (a), the strobe plot of (d), and the power spectrum of (g), which are fully in agreement with Figures 3a, 4a

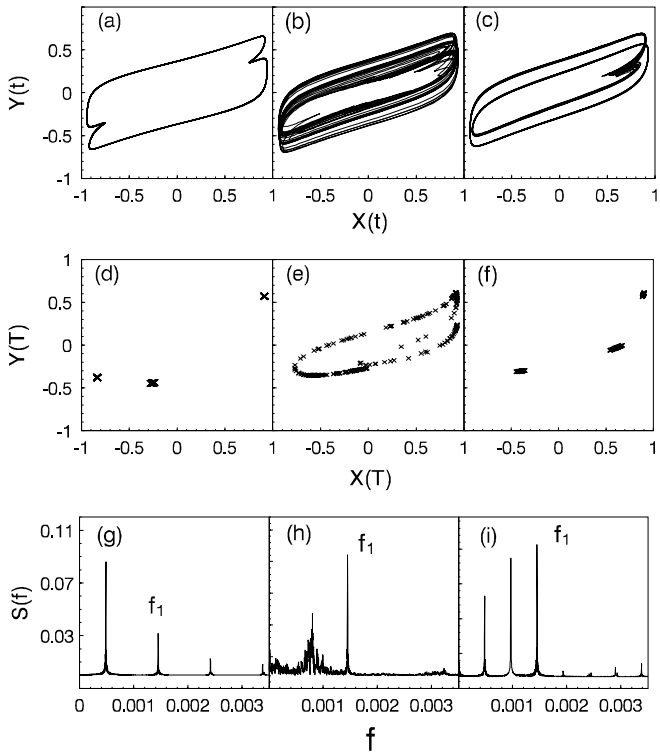

Fig. 9. The same as Figure 8 with $N = 100$.

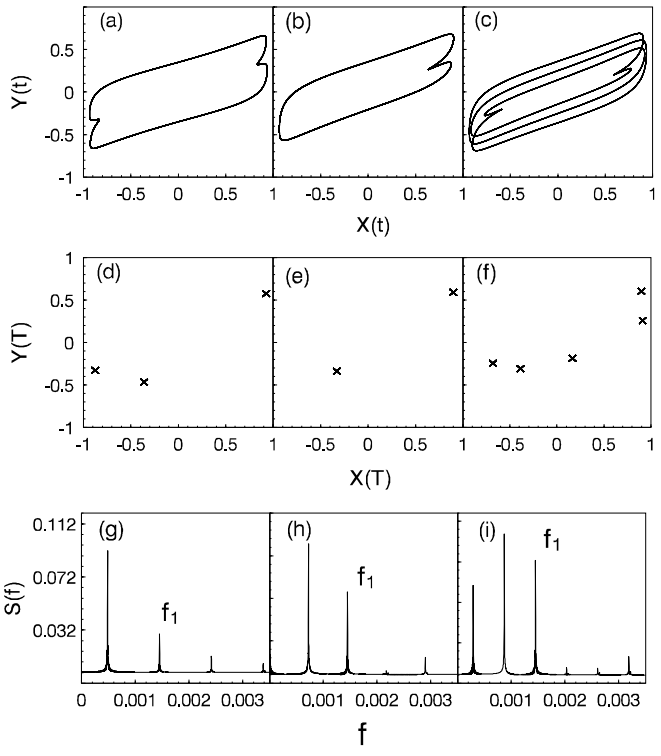

Fig. 10. The same as Figure 8 with $N = 10^4$.

and 5a, respectively. Thus, equations (8) produce qualitatively correct behavior of equations (4). However, fluctuation caused by the finite system size destroys P_2^1 (referring to (b) in Figs. 3–5), and only a small trace of $\frac{1}{2}f_1$ can be found in the spectrum of Figure 9h. In Figures 9c, f and i one can observe P_3^1 motion, while for the same parameters the motion of equations (8) was P_5^2. Therefore, finite system size can shift the bifurcation diagram of the coupled system.

Increasing N further, we find: the larger the system size (N), the weaker the fluctuations are due to finite system size, so more numerous sharper bifurcations can survive, and the better equations (8) can represent equations (4). In order to show the rich bifurcations clearly and in the same location as in Figures 3–5, the finite system should have no less than 10^4 cells. In Figure 10, we show the three subharmonics of $N = 10^4$, and they are all consistent with those in Figures 3–5.

In Figure 11, we directly compute the original system, (Eqs. (2)), for $N = 10^4$. We find a number of subharmonics like period-three, period-four, and period-five, represented by the corresponding strobe plots and spectra; these confirm the existence of noise-induced complexities. However, the parameter values for various subharmonics for equations (2) are distinguished from those for (8). This is due to the fact that condition (3) is invalid since the D and μ values for the given subharmonics are no longer small.

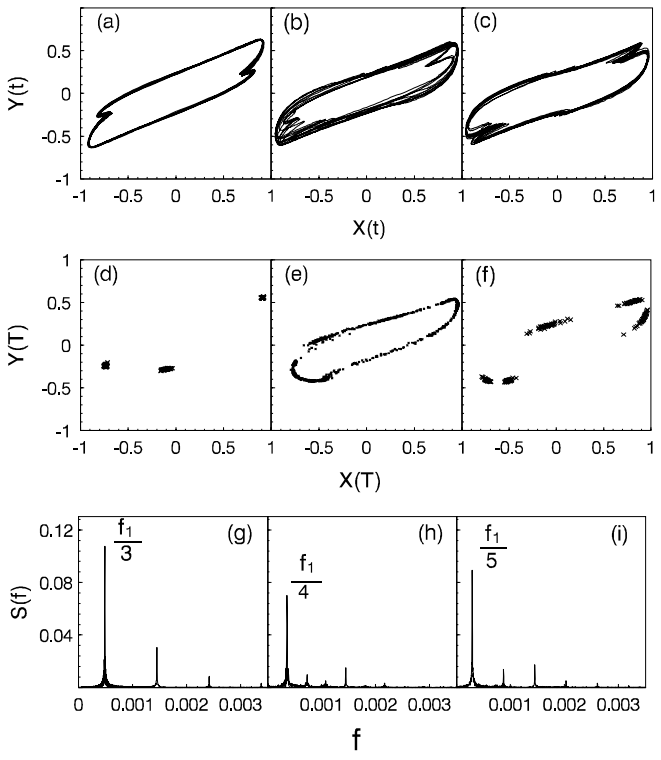

Fig. 11. (a–c) Orbits from the simulation of equation (2). $N = 20000$, $\mu = 0.16$. (d–f) Strobe plots corresponding to (a–c). (g–i) Frequency spectra corresponding to (a–c). (a, d, g) show period three oscillation with $D = 0.043$; (b, e, h) show period four oscillation with $D = 0.0402$; (c, f, i) show period five oscillation with $D = 0.039$.

5 Conclusion

In summary, we have investigated noise-induced bifurcation behavior of the average motion in globally coupled stochastic oscillators. Large numbers of coupled Langevin equations, which consist of two kinds of competing cells under small periodic forcing, are considered. With infinite size limit, the coupled master equations simplified from the model can be reduced to a set of two-dimensional differential equations. The reduced system exhibits a simple behavior for either very small or rather large noise intensity, but for an intermediate D, considerable complex behavior appears. Rich bifurcations to subharmonics induced by noise exist and they array in the Farey tree. If the periodic forcing A is not too weak, chaos can be induced by noise and there are three routes for the transition into chaos, *i.e.*, tangent bifurcation to chaos, periodic doubling cascade to chaos, and quasiperiodicity to chaos. If the forcing is too weak, a quasiperiodic sea and phase locking tongues are observed.

In addition, the influence of a finite system size is considered. It is found that infinitely sharp bifurcations can be found only in the limit $N \to \infty$. This is similar to the phase transitions in equilibrium states. Nevertheless, various complexities revealed for $N \to \infty$ can be still observed for finite systems, though reducing system size can smoothen sharpness of bifurcations, rule out subharmonics with high periods and shift the locations of various subharmonics in the parameter space. Of course, very small N would certainly wipe away the fine structures entirely, and produce only trivial behavior of periodically driven random motion.

We come to the conclusion that noise can induce complicated bifurcations to subharmonics and chaos in the extended system under thermodynamic limit, and these noise-induced complexities still survive for practically large though finite systems.

This work is supported by the National Science Foundation of China, N19835020, Nonlinear Science Project, and Doctoral Program Foundation of Institute of Higher Education.

References

1. R. Benzi, A. Sutera, A. Vulpiani, J. Phys. A **14**, L453 (1981).
2. P. Jung, P. Hanggi, Europhys. Lett. **8**, 505 (1989).
3. G. Hu, G. Nicolis, C. Nicolis, Phys. Rev. A **42**, 2030 (1990).
4. M.I. Dykman, R. Mannella, P.V.E. McClintock, N.G. Stocks, Phys. Rev. Lett. **68**, 2985 (1992).
5. P. Jung, U. Behn, E. Pantazelou, F. Moss, Phys. Rev. A **46**, R1709 (1992).
6. J.L. Douglass, L. Wilkens, E. Pantazelou, F. Moss, Nature **365**, 337 (1993).
7. J.J. Collins, C.C. Chow, T.T. Imhoff, Nature **376**, 236 (1995).
8. F. Marchesoni, L. Gammaitoni, A.R. Bulsara, Phys. Rev. Lett. **76**, 2609 (1996).
9. M. Locher, G.A. Johnson, E.R. Hunt, Phys. Rev. Lett. **77**, 4698 (1996).
10. P. Jung, K. Wiensenfeld, Nature **385**, 291 (1997).
11. L. Gammaitoni, P. Hanggi, P. Jung, F. Marchesoni, Rev. Mod. Phys. **70**, 223 (1998).
12. B. McNamara, K. Wiesenfeld, Phys. Rev. A **39**, 4853 (1989).
13. Y. Zhang, G. Hu, H. Liu, J.H. Xiao, Phys. Rev. E **57**, 2543 (1998).
14. G. Hu, H. Haken, F. Xie, Phys. Rev. Lett. **77**, 1925 (1996).
15. J. Xiao, G. Hu, H. Liu, Y. Zhang, Eur. Phys. J. B **5**, 133 (1998); H. Liu, G. Hu; Y. Zhang, J.H. Xiao, Commun. Theor. Phys. **33**, 191 (2000).